

Symmetry of excitons in GaN

R. Stępniewski

Institute of Experimental Physics, Warsaw University, Hoża 69, PL-00-681 Warszawa, Poland

M. Potemski

Grenoble High Magnetic Field Laboratory, MPI/FKF-CNRS, Boîte Postale 166X, F-38042 Grenoble Cedex 9, France

A. Wysmołek, K. Pakuła, and J. M. Baranowski

Institute of Experimental Physics, Warsaw University, Hoża 69, PL-00-681 Warszawa, Poland

J. Łusakowski

Grenoble High Magnetic Field Laboratory, MPI/FKF-CNRS, Boîte Postale 166X, F-38042 Grenoble Cedex 9, France

I. Grzegory and S. Porowski

High Pressure Research Center, Polish Academy of Sciences, Sokolowska 29/37, PL-01-142 Warszawa, Poland

G. Martinez and P. Wyder

Grenoble High Magnetic Field Laboratory, MPI/FKF-CNRS, Boîte Postale 166X, F-38042 Grenoble Cedex 9, France

(Received 7 April 1999)

Magnetorefectivity measurements on GaN are used to resolve the symmetry of three excitonic resonances, arising from the crystal-field and spin-orbit effects on the valence band. The symmetry characteristic for each valence subband is directly seen in the observed Zeeman pattern. The linear magnetic-field effect for all exciton components is well accounted for by introducing only two coupling constants: the electronic g factor for the conduction band and the Luttinger κ parameter for the valence band. The strength of the electron-hole exchange interaction is determined. [S0163-1829(99)08531-8]

In most semiconductors, excitonic resonances involve a coupled pair of an s -type conduction-band electron and a p -type valence-band hole. The behavior of this 12-fold degenerate exciton ground state in the presence of spin-orbit interaction, crystal field, electron-hole exchange, and a magnetic field is a challenge for the Luttinger model,¹ which accounts for the complex nature of valence-band states. In this model, the effects of a magnetic field are taken into account in terms of a single coupling constant (κ), which redefines the g factors for different valence subbands. A single κ model has been successfully introduced for the four-fold degenerate $J=3/2$ hole subbands in zinc-blende semiconductors.^{2,3} On the other hand, in the case of lower-symmetry, wurtzite-type semiconductors, the magnetic field pattern of different excitonic states has only been discussed in terms of the effective g factors, separately for each valence subband.^{4,5} Such a many-parameter description offers a rather limited understanding of excitonic resonances, particularly in the case when the amplitudes of spin-orbit and crystal-field interactions are of the same order. GaN is a representative wurtzite structure semiconductor with comparable strength of spin-orbit and crystal-field interactions.⁶ It is a technologically important compound because of the relevant efforts to “blue-shift” the spectral range of optoelectronic semiconductor devices, though its optical properties are still not sufficiently known.⁷ It is clear, however, that the near band edge response in this material is determined by the so called A , B , and C exciton components which are close in energy and most likely form a coupled state, and therefore

need to be understood within the most general model possible with a minimum number of parameters.

In this paper we examine the symmetry of excitons in wurtzite structure GaN crystals using high field magnetorefectance experiments. The magnetic-field pattern of the resonances is confronted with calculations based on the Luttinger model completed by introducing the crystal-field and electron-hole exchange interactions. We show that symmetries of the observed magneto-excitonic levels can be satisfactorily parametrized using only two coupling constants, i.e., the g factor for the conduction band-electrons and a single κ parameter for all three valence subbands. The interplay between the crystal-field and spin-orbit interactions leads to the unexpected spin symmetries of the resulting exciton states. The experimental observations are well accounted for by the invariant expression for a Hamiltonian based on group theory.

The experiments were performed using homoepitaxial GaN layers grown by metal-organic chemical-vapor depositive (MOCVD) on GaN bulk crystals. A detailed description of samples and the experimental setup is given elsewhere.⁶ Low temperature reflectivity spectra were measured with the magnetic field \mathbf{B} parallel and perpendicular to the \mathbf{c} axis of the GaN crystal lattice. The representative raw data measured in the configuration of the magnetic field $\mathbf{B} \parallel \mathbf{c}$, in the range from $\mathbf{B}=0$ to 27 T, are presented in Fig. 1. The spectrum obtained at $\mathbf{B}=0$ shows three characteristic features, which correspond to the optically active excitons A , B , and C . This is typical for wurtzite structure semiconductors⁸

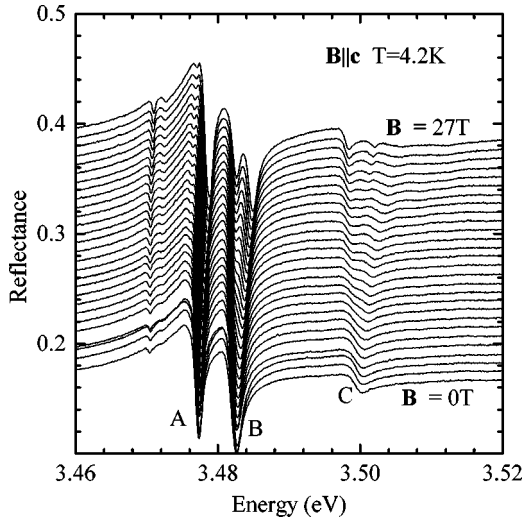


FIG. 1. Magnetorefectance spectra of GaN measured in magnetic fields up to 27 T applied along the c axis of the wurtzite crystal. For clarity, subsequent spectra are shifted vertically.

and directly reflects the valence-band splitting caused by the spin-orbit and crystal-field interactions. The magnetic-field evolution of the reflectivity spectra shows the Zeeman effect which is essentially different for different exciton components and also depends on the magnetic-field orientation. For example, in the $\mathbf{B}\parallel\mathbf{c}$ configuration (see Fig. 1) we clearly observe the spin splitting of B and C excitons, while exciton A does not split in this configuration, though a tiny feature appears on its low energy wing.⁹

The energy positions of the excitonic resonances have been defined from the measurements by the standard method of calculating the derivatives, dR/dE , of the reflectivity spectra and assigning the maxima of $(-dR/dE)$ to the optically active transverse excitons. This method can introduce some systematic error in the absolute value of the exciton energy, but is quite accurate in describing the relative displacement of the Zeeman components. The energy positions of the exciton Zeeman components, measured for different magnetic fields and for two experimental configurations are shown in Fig. 2. Representative derivatives of the reflectance spectra measured at $B=27$ T are also presented in this figure. Using the “derivative” method we can very easily follow the magnetic field evolution of excitons A and B . This procedure is less effective in the region of exciton C because of the significant broadening of this resonance and because of the overlap of exciton C with the excited states of excitons A and B . Nevertheless, the effect of magnetic fields on exciton C can be quite clearly seen in the raw data (see Fig. 1). Note, for example, that exciton C splits into only two components in the $\mathbf{B}\parallel\mathbf{c}$ configuration whereas the feature appearing in between the two spin-split components [see Fig. 2(a)] is related to the $2s$ state of exciton A .

We note the following characteristic features of splitting patterns presented in Fig. 2(a) and 2(b). (i) $\mathbf{B}\parallel\mathbf{c}$ configuration: the spin splitting of exciton A is negligibly small;¹⁰ exciton B splits into two components of comparable intensities; the biggest splitting is observed for exciton C . (ii) $\mathbf{B}\perp\mathbf{c}$ configuration: the exciton A clearly splits into two components; exciton B shows up to four spin-split components at highest fields; exciton C splits into more than two optically

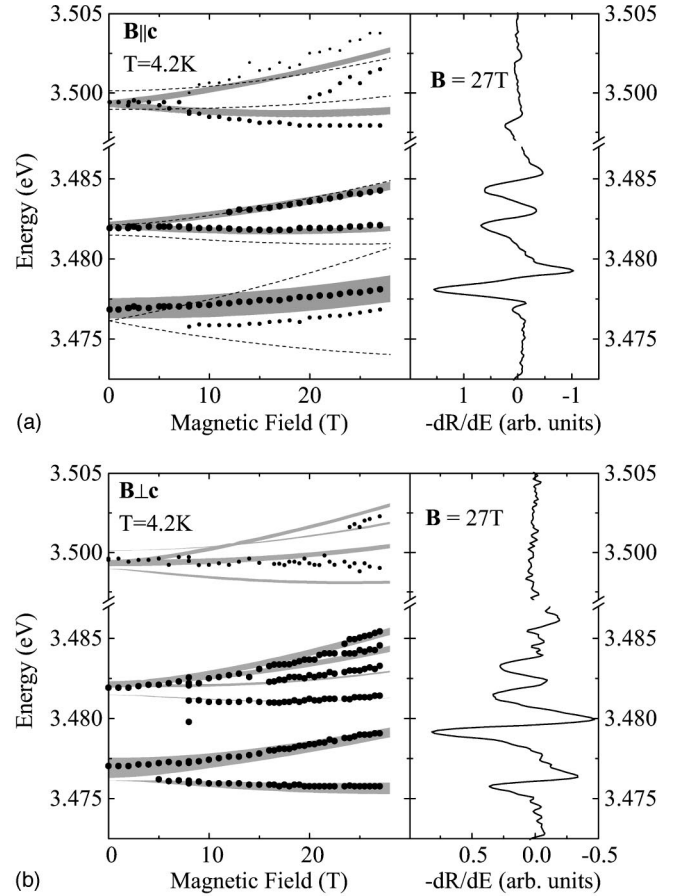


FIG. 2. (a) Left side: energies of the Zeeman components for the exciton in GaN as a function of the magnetic field for $\mathbf{B}\parallel\mathbf{c}$; circles – experiment; shadow and broken lines – calculated energies of optically active and “dark” excitons, respectively. The width of the shadow area is proportional to the calculated oscillator strength of a given Zeeman component. Right side: derivative of the reflectance spectrum at $B=27$ T. (b) The same as (a) for the magnetic-field direction $\mathbf{B}\perp\mathbf{c}$.

active components (due to a broadening and the appearance of the excited states of exciton A , the splitting pattern of exciton C is less precisely determined).

These observations allow us to deduce the symmetry breaking diagram of the sixfold degenerate valence band and the twofold degenerate conduction band states. Such a diagram, reflecting the simplified approach to excitonic transitions in terms of band-to-band transitions, is schematically shown in Fig. 3. Within this approach, the symmetry of each exciton component is characterized by two quantum numbers (s_e, j_z) . $s_e = \pm 1/2$ and $j_z = \pm 3/2, \pm 1/2$ denote, respectively, the projections of the conduction-band spin and of the total angular momentum of the valence-band states onto the direction parallel to the c axis of the crystal. As shown in Fig. 3, the spin-orbit and crystal-field interactions reduce the high symmetry of initial states to those with $\Gamma_9(j_z = \pm 3/2)$ and $\Gamma_7(s_e = \pm 1/2$ or $j_z = \pm 1/2)$ symmetries. The orientation of the magnetic field with respect to the crystal c axis is an important ingredient in the determination of a transition’s symmetry: states with Γ_7 symmetry split in both configurations of the magnetic field whereas the states of Γ_9 symmetry split in the $\mathbf{B}\parallel\mathbf{c}$ configuration but not when $\mathbf{B}\perp\mathbf{c}$.⁸

Our results confirm the $\Gamma_9 \rightarrow \Gamma_7$ character of the transition

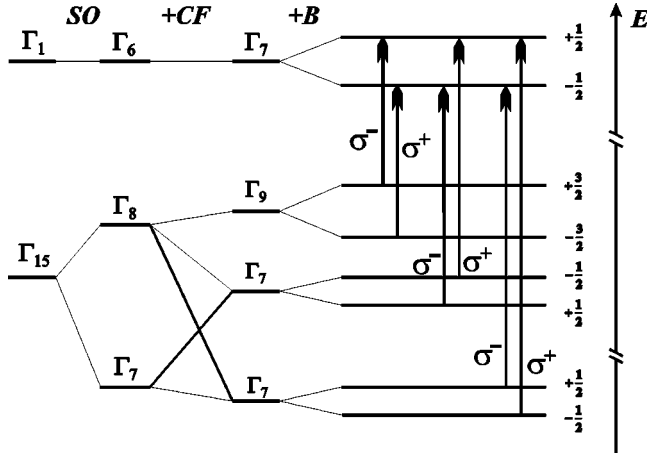


FIG. 3. Breaking symmetry scheme of the conduction and valence bands in GaN. The influence of the subsequent interactions: spin-orbit, crystal-field, and the magnetic-field ($\mathbf{B}\parallel\mathbf{c}$) is shown from left to right. The total angular momentum of the resulting states is given on the right side. The optically active excitons correspond to the allowed transitions, which are marked by arrows.

associated with exciton A. As expected, this transition shows only two, equal intensity Zeeman components in the $\mathbf{B}\perp\mathbf{c}$ configuration. The splitting of exciton A in this configuration is determined solely by the spin splitting in the conduction band, allowing a direct measure of the electron g_e factor. In the $\mathbf{B}\perp\mathbf{c}$ configuration one expects up to four Zeeman components for each $\Gamma_7\rightarrow\Gamma_7$ interband transition, as indeed is observed for excitons B and C.

The case of the $\mathbf{B}\parallel\mathbf{c}$ configuration is particularly transparent due to the clearly defined $s_e-j_z=\pm 1$ selection rules for optically allowed transition (see Fig. 3). In this configuration, each exciton A, B, and C is expected to split into a doublet. Apparently, the spin splitting of the $\Gamma_9\rightarrow\Gamma_7$ transition is not experimentally resolved. This is because spin splittings in the conduction and the valence band compete with each other leading to an almost exact cancellation of the Zeeman effect for the exciton A in this configuration. We assume that $g_e > 0$ and that its value is not sensitive to the field orientation,¹¹ therefore concluding that the g factor value for the Γ_9 valence-band states is positive: $g_{vA}\parallel\approx g_e > 0$.

Although exciton A remains accidentally degenerate when $\mathbf{B}\parallel\mathbf{c}$, the doublet splitting is indeed observed for excitons B and C. We note that the spin splitting of exciton B in the $\mathbf{B}\parallel\mathbf{c}$ configuration is smaller than the spin splitting of exciton A in the $\mathbf{B}\perp\mathbf{c}$ configuration, the latter splitting being determined solely by the spin splitting in the conduction band. According to the selection rules shown in Fig. 3, we conclude that the g factor of Γ_7 valence states associated with exciton B is negative ($g_{vB}\parallel < 0$). In contrast, the spin splitting of exciton C in the $\mathbf{B}\parallel\mathbf{c}$ configuration is bigger than the spin splitting in the conduction band and therefore the g factor of Γ_7 valence states associated with exciton C is positive ($g_{vC}\parallel > 0$). The resulting spin order of Zeeman components of the valence states is shown in Fig. 3.

It is interesting to note that in the limit of the finite spin-orbit splitting ($\Delta_{so} > 0$) but vanishing crystal field effect ($\Delta_{cf} = 0$), one would expect¹ that $g_{vB}\parallel^0 = \frac{1}{3}g_{vA}\parallel > 0$ and $g_{vC}\parallel^0 = (\frac{1}{3}g_{vA}\parallel - 1) < 0$ in contrast to our observation ($g_{vB}\parallel < 0$,

$g_{vC}\parallel > 0$). Although the crystal-field effects are relatively weak in GaN ($\Delta_{so} > \Delta_{cf}$),⁶ our results clearly show that mixing of valence-band states in this compound is sufficiently strong to reverse the spin order for the two Γ_7 valence subbands.

The qualitative considerations presented above can be justified by comparing the experimental data with the following, more rigorous model. We assume that the 12-fold degenerate ground exciton is composed of an s -like conduction-band electron and a p -type valence-band hole, which can be described using a $|s_e, l_z, s\rangle$ basis, where the z direction is chosen along the \mathbf{c} axis. These three quantum numbers correspond to the spin operator of the electron $\vec{s}_e (s_e = \pm \frac{1}{2})$, orbital angular momentum, and spin operators of the hole $\vec{l} (l_z = 1, 0, -1)$ and $\vec{s} (s = \pm \frac{1}{2})$, respectively. For the wurtzite structure, in the simplest, quasicubic approximation, neglecting the k dispersion, an invariant expression of the $1s$ exciton Hamiltonian for $\mathbf{B} = 0$ gives:^{12,13}

$$H_0 = E_0 - \Delta_{cf} l_z^2 - \frac{2}{3} \Delta_{so} \vec{l} \vec{s} + 2 \Delta_{ex} \vec{s}_e \vec{s}, \quad (1)$$

where E_0 corresponds to the energy gap; Δ_{cf} and Δ_{so} denote, respectively, the crystal-field and spin-orbit splittings, and Δ_{ex} is the isotropic exchange splitting. The values of the crystal-field and spin-orbit interaction parameters determine the Γ_9 , Γ_7 , and Γ_7 energies of the split valence bands.⁶

According to Luttinger,¹ the linear magnetic-field effects can be included as follows:

$$H_B = g_e \mu_B \vec{B} \vec{s}_e + 2 \mu_B \vec{B} \vec{s} - \mu_B (3\tilde{\kappa} + 1) \vec{B} \vec{l}. \quad (2)$$

Here, the first term corresponds to the Zeeman splitting of the conduction band and is described by the effective g factor of the electron g_e . The next two terms account for the valence subbands splitting and are related to the spin and orbital angular momentum of the hole, respectively. The parameter $\tilde{\kappa}$ gives directly the Zeeman splitting of the hole bound in exciton A for the $\mathbf{B}\parallel\mathbf{c}$ configuration ($g_{hA}\parallel = 6\tilde{\kappa}$).¹⁴ Its value may be directly expressed by the κ parameter of the free hole, and other valence-band parameters.^{2,15} The diamagnetic shift, clearly visible in the experimental results (Fig. 2), was introduced in the simplest way through $H_D = d\mathbf{B}^2$.

When the direction of the incoming light is normal to the crystal surface, the following four states among exciton basis are optically active: $|+\frac{1}{2}, \pm 1, -\frac{1}{2}\rangle$ and $|-\frac{1}{2}, \pm 1, +\frac{1}{2}\rangle$. For the unpolarized light their oscillator strengths are equal.

The diagonalization of the Hamiltonian $H = H_0 + H_B + H_D$ gives the energies and eigenfunctions of the exciton Zeeman components, and their oscillator strengths can be calculated. The resulting exciton spectrum is presented in Fig. 2 in comparison with the experimental results. Four eigenstates of the Hamiltonian with the lowest energy correspond to the components of exciton A. For the magnetic field $\mathbf{B}\parallel\mathbf{c}$, two of them, with Γ_5 symmetry, are almost pure basis states, namely $|+\frac{1}{2}, -1, -\frac{1}{2}\rangle$ and $|-\frac{1}{2}, +1, +\frac{1}{2}\rangle$, and are optically active.⁵ For this configuration, the magnetic-field-

TABLE I. Band structure parameters of GaN obtained from the analysis of the near band edge magnetorefectance, and the resulting energies of the optically active excitons for $B=0$.

Δ_{cf} (meV)	Δ_{so} (meV)	Δ_{ex} (meV)	g_{el}	$\tilde{\kappa}$	d ($\mu\text{eV}/\text{T}^2$)	E_A (meV)	E_B (meV)	E_C (meV)
10.2 ± 0.1	18.1 ± 0.2	-0.91 ± 0.05	1.94 ± 0.02	-0.36 ± 0.01	1.84 ± 0.1	3476.9 ± 0.3	3482.1 ± 0.3	3499.3 ± 0.8

induced splitting between these states is equal to $\Delta_{A\parallel}(B) = |(g_e + 6\tilde{\kappa})\mu_B B|$. Since this splitting is not resolved, one can estimate $\tilde{\kappa} \approx -g_e/6$.

Two other eigenstates: $|-\frac{1}{2}, -1, -\frac{1}{2}\rangle$ and $|+\frac{1}{2}, +1, +\frac{1}{2}\rangle$ belong to ‘‘dark excitons’’ with Γ_6 symmetry. A magnetic field applied in the direction perpendicular to the \mathbf{c} axis introduces coupling between the optically active and ‘‘dark’’ A excitons. In the first approximation, neglecting the interactions with excitons from the B and C groups, the observed splitting is described by⁸ $\Delta_{A\perp}(B) = \sqrt{\Delta_{ex}^2 + (g_e\mu_B B)^2}$.

Thus, the zero-field exciton energies, A -exciton diamagnetic shift, and its splitting measured for two configurations $\mathbf{B}\parallel\mathbf{c}$ and $\mathbf{B}\perp\mathbf{c}$, give sufficient information to estimate all parameters involved in the above Hamiltonian. Finally their values have been corrected using a least-squares-fit procedure taking into account all transitions resolved in the experiments (see Fig. 2). The obtained parameter values are listed in Table I.

Our model is in fair agreement with the experimental results presented in Figs.2(a) and 2(b). Some disagreement observed for the exciton C can be related to its interferences with the excited states of excitons A and B . The resulting spin-splitting pattern of excitons A , B , and C (see Fig. 3), allows us to determine the symmetry breaking scheme of the corresponding valence states. The nonintuitive spin ordering for the two Γ_7 valence states is an interesting consequence of the valence-band mixing. The coupling constant $\tilde{\kappa}$ was determined in GaN for the first time. The electron-hole exchange interaction is quite important in this compound due to

a strong localization of the exciton wave functions. The g factor value of the electron involved in the free exciton is, within experimental error, the same as obtained for the shallow donor¹¹ $g_D=1.95$. The crystal-field parameter, $\Delta_{cf}=10.2$ meV, presented here differs from the value of 8.8 meV reported previously,⁶ since in Ref. 6 the exchange interaction was not taken into account, and since the exciton energies may differ slightly among different samples due to a small residual strain.

In conclusion, reflectivity measurements in high magnetic fields were used to study the free exciton symmetry in GaN. We have shown that a quite complicated Zeeman splitting pattern, observed for the free exciton states in a wurtzite symmetry semiconductor, can be well approximated using the classical Luttinger model with a single coupling constant κ for all three valence-band components. The competition between the spin-orbit and crystal-field interactions leads to an unexpected sequence of the g factor signs for the valence subbands. The obtained band structure parameters substantially improve the state of knowledge about this important wide gap semiconductor.

This work was partially supported by the State Committee for Scientific Research (Republic of Poland) Grants No. PBZ 08-11 and 2 P03B 038 15. The Grenoble High Magnetic Field Laboratory is associated with the INPG and University Joseph Fourier de Grenoble. A.W. acknowledges the Alexander von Humboldt Foundation and two of us (R.S. and K.P.) acknowledge Lepton Ltd. for financial support.

¹J.M. Luttinger, Phys. Rev. **102**, 1030 (1956).

²D. Bimberg, Festkoerperprobleme **XVII**, 195 (1977).

³H. Venghaus, S. Suga, and K. Cho, Phys. Rev. B **16**, 4419 (1977).

⁴I. Broser and M. Rosenzweig, Phys. Rev. B **22**, 2000 (1980); M. Rosenzweig, Phys. Status Solidi A **129**, 187 (1985).

⁵G. Blattner, G. Kurtze, G. Schmieder, and C. Klingshirn, Phys. Rev. B **25**, 7413 (1982).

⁶R. Stępniewski, K.P. Korona, A. Wyszkołek, J.M. Baranowski, K. Pakuła, M. Potemski, G. Martinez, I. Grzegory, and S. Porowski, Phys. Rev. B **56**, 15 151 (1997).

⁷For a review see F.A. Ponce and D.P. Bour, Nature (London) **386**, 351 (1997); for details, see S. Nakamura and G. Fasol, *The Blue Laser Diode: GaN based Light Emitters and Lasers* (Springer-Verlag, Heidelberg, 1997).

⁸D.G. Thomas and J.J. Hopfield, Phys. Rev. **128**, 2135 (1962).

⁹We do not discuss in this paper the weak structure at 3.471 eV, attributed to a donor bound exciton.

¹⁰In the case of the exciton A for $\mathbf{B}\parallel\mathbf{c}$ configuration, the proper

interpretation of the reflectivity spectrum requires a numerical analysis, in which the polariton effects are taken into account [J. Lagois, Phys. Rev. B **16**, 1699 (1977)]. It was checked by numerical simulation [K.P. Korona (unpublished)] that the appearance of a tiny structure on the lower energy side of the main line is due to Zeeman splitting of exciton A , which is smaller than 0.8 meV at 27 T.

¹¹W.E. Carlos, J.A. Jr. Freitas, M. Asif Khan, D.T. Olson, and J.N. Kuznia, Phys. Rev. B **48**, 17 878 (1993).

¹²G.L. Bir and G.E. Pikus, in *Symmetry and Strain-Induced Effects in Semiconductors* (Halsted, Jerusalem, 1974).

¹³J. Wrzesinski and D. Fröhlich, Solid State Commun. **105**, 301 (1998).

¹⁴Note that the electron g factor has a sign opposite to that of the corresponding hole ($g_{vA\parallel} = -g_{hA\parallel}$, etc.).

¹⁵A.V. Malyshev, I.A. Merkulov, and A.V. Rodina, Phys. Solid State **40**, 917 (1998) [Fiz. Tverd. Tela (St. Petersburg) **40**, 1002 (1998)].